Enhanced Hole Mobility in Poly-(2-methoxy-5-(2′-ethylhexoxy)-1,4-phenylenevinylene) by Elimination of Nanometer-Sized Domains**

By *Anto Regis Inigo*, *Chia Cheng Chang*, *Wunshain Fann*,* *Jonathon David White*, *Ying-Sheng Huang*, *U.-S. Jeng*, *Hwo Shuenn Sheu*, *Kang-Yung Peng*, and *Show-An Chen*

Optoelectronic devices based on conjugated polymer thin films are attractive owing to their low cost and ease of processing.[1–3] Charge-carrier mobility, directly related to the order/disorder present in the material, currently limits many potential applications. Methods capable of improving polymer morphology and hence mobility are thus of considerable interest not only scientifically but also technologically. One focus of current research has been on increasing intermolecular order. The development of ordered crystal-like films of up to macroscopic size has been successful in improving charge-transport characteristics (i.e., mobility) in poly(thiophene) derivatives.[4,5] The large mobility increase recently obtained in ladder-type polymers (i.e., from 4×10^{-6} $cm^2\,V^{-1}\,s^{-1}$ to 0.1 $cm^2\,V^{-1}\,s^{-1}$ in poly(benzobizimidobenzophenonthroline) (BBL)) is at least partly the result of morphological changes which provided greater intermolecular order (as proved by atomic force microscopy and X-ray diffraction).[6,7] In this Communication, we demonstrate that mobility can also be improved by an order of magnitude, not by increasing intermolecular order, but rather by eliminating nanometer-sized crystal formation.

One of the most studied of the poly(phenylenevinylene) (PPV)-derivative polymers is poly(2-methoxy-5-(2′-ethylhexoxy)-1,4-phenylenevinylene) (MEH-PPV). A soluble derivative of PPV, it has a variety of conformations depending upon its intrinsic chemical properties and processing conditions.[8–10] Much research has focused on understanding the relationships between morphology and luminescence properties.[11–13] Morphology variation can lead to different kinds of charge-carrier transport, ranging from highly dispersive to non-dispersive.[14,15] Using different solvents (i.e., toluene (TL) and chlorobenzene (CB)), we demonstrated that TL-cast MEH-PPV films have a larger ordered domain size but fewer domains than CB-cast MEH-PPV films. The mobility in TL-cast films was found to be higher than that of CB-cast films.[16] These results suggest that mobility might be further enhanced by reducing the density of nanometer-sized domains in polymer films.

In this work, thin films were prepared using the drop-casting method from 5 $mg\,mL^{-1}$ of MEH-PPV in CB on indium tin oxide (ITO)-coated substrates. During the deposition process, in one group of films, an electric field (E_{cast}) was applied parallel to the substrate in order to inhibit domain formation (these are henceforth denoted "E-field-cast"). A second group of films (henceforth denoted "as-cast") served as a control group in which no electric field was applied during deposition. Figure 1 shows time-of-flight (TOF) photocurrent transients in linear scale (inset, log–log scale) recorded at 295 K for as-cast (Fig. 1a) and E-field-cast (Fig. 1b) films. The transit times were obtained from the $\log(i)-\log(t)$ plot. The transit time in the E-field-cast device is much shorter than for the as-cast device. Hole mobility (μ) in the E-field-cast device is thus greater than in as-cast devices ($\mu = d/E\ t_{tr}$ where E is the bias field, t_{tr} is the transit time and d is the thickness of polymer film).

Figure 2 gives the field-dependent mobility at room temperature. The mobilities in the E-field-cast film are consistently one order of magnitude higher than the as-cast films. While all measured mobilities follow the Poole–Frenkel relationship,

$$\ln(\mu(E)/\mu_{E=0}) = S\,E^{1/2} \quad (1)$$

(where E is an externally applied electric field, S is the slope of the field-dependent mobility, and $\mu_{E=0}$ is the zero-field mobility), the slopes are higher for the E-field-cast devices than for the as-cast devices. This indicates that the positional disorder present in the as-cast devices is larger than in the E-field-cast devices, and that the positional disorder seems to dominate charge-transport characteristics.[17] The field-dependent mobility for different temperatures in as-cast and E-field-cast films was also measured at 10 K intervals as shown in Figure 2b. For as-cast films, there is a gradual variation of

[*] Prof. W. Fann, Dr. A. R. Inigo
Institute of Atomic and Molecular Sciences, Academia Sinica
P. O. Box 23-166, Taipei 106 (Taiwan)
E-mail: fann@gate.sinica.edu.tw
Prof. W. Fann
Department of Physics and Institute of Polymer Sciences and Engineering
National Taiwan University
Taipei 106 (Taiwan)
C. C. Chang
Department of Physics and Institute of Polymer Sciences and Engineering
National Taiwan University
Taipei 106 (Taiwan)
Prof. J. D. White
Department of Electrical Engineering, Yuan Ze University
Neili, Taoyuan 320 (Taiwan)
Prof. Y.-S. Huang
Department of Electronic Engineering
National Taiwan University of Science and Technology
Taipei 106 (Taiwan)
Dr. U.-S. Jeng, Dr. H. S. Sheu
National Synchrotron Radiation Research Center
Hsinchu 300 (Taiwan)
Dr. K.-Y. Peng, Prof. S.-A. Chen
Department of Chemical Engineering, National Tsing Hua University
Hsinchu 300 (Taiwan)

[**] This research is supported by Academia Sinica and MOE Program for Promoting Academic Excellence of Universities (grant number 91-E-FA04-2-4A) and by National Science Council (grant number 93-2120M-002-009). We acknowledge the stimulating discussions had with Prof. A. C. Su.

 DOI: 10.1002/adma.200500331

ADVANCED MATERIALS

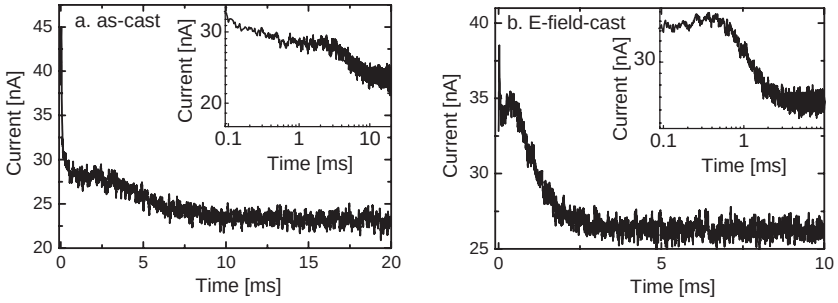

Figure 1. TOF photocurrent transients for as-cast (a) and E-field-cast (b) thin films at 295 K for a 100 kV cm^{-1} applied electric field. The main figures display data with a linear scale while the insets are log(*i*)–log(*t*) plots. Film thickness was 3.6 μm for the E-field-cast device and 3.5 μm for the as-cast device as measured by a surface profile meter. The residual current is the result of a direct-current (DC) component that is not subtracted from the background.

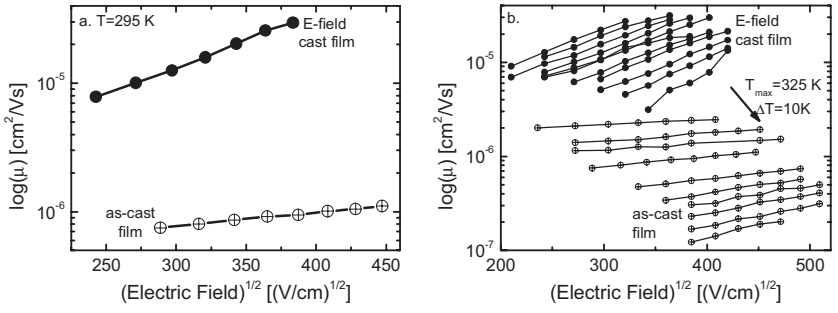

Figure 2. a) Field-dependent mobility for as-cast and E-field-cast devices at room temperature. b) The temperature dependence of field-dependent mobility for as-cast and E-field-cast devices.

the slope as the temperature increases from 225 K to 325 K. In contrast, for E-field-cast films, there is no significant change of slope. This also indicates that the positional disorder present in the E-field-cast films is less than that in the as-cast films.[17]

Bässler proposed a model which he named the Gaussian Disorder Model (GDM).[17] In GDM, two parameters, energy disorder (σ) and positional disorder (Σ), are used for specifying the disorder present in the materials. Energy disorder describes the distribution of energy levels associated with transport. Positional disorder describes the fluctuation in the distance and orientation of the hopping sites associated with the hopping carriers. Both parameters are influenced by material morphology which depends not only on chemical structure but also on processing conditions such as temperature treatment and solvent.[15] This model has been extended to accommodate large hopping distances and long-chain polymers by introducing spatial correlations of energy levels of charge carriers.[18,19] Both of these models, GDM and correlated GDM, have been used as an aid in understanding the nature of charge transport and other physical parameters in MEH-PPV, other PPV derivatives, and ladder-type PPV.[20–23]

We chose to analyze the mobility results using the relationship developed in GDM, namely:

$$\mu(E,T,\sigma,\Sigma) = \mu_0 \exp -\left(\frac{2\sigma}{3k_B T}\right)^2 \times \exp\left(C\left(\frac{\sigma}{k_B T}\right)^2 - \Omega\sqrt{E}\right) \quad (2)$$

where μ_0 is the mobility at infinite absolute temperature and zero field, T is the absolute temperature (K), k_B is the Boltzmann constant, and C is an empirical constant (C is expected to scale with the square root of the intermolecular distance and equals 2.9×10^{-4} (cm V^{-1})$^{1/2}$ for an average intermolecular distance of 6 Å). Ω is defined as follows: if $\Sigma > 1.5$, $\Omega = \Sigma^2$, otherwise $\Omega = 2.25$. The energy-disorder parameters obtained by plotting $\ln(\mu(E=0))$ against $1/T^2$ (Fig. 3a) are 86 and 71 meV for the as-cast and E-field-cast films, respectively. The positional disorder parameters obtained by plotting the slop of the field-dependent mobility against the square of the normalized energy disorder (σ/kT), are 3.60 and < 1.5 for the as-cast and E-field-cast films, respectively (Fig. 3b). Compared to as-cast films, E-field-cast films are characterized by a smaller positional and energy disorder, which reflects a decrease in the fluctuation of the separation and orientation of hopping sites.

In order to understand the underlying reasons for the enhanced mobility in the E-field-cast films, we investigated the underlying morphological differences between the two types of films using wide-angle X-ray scattering (WAXS). In Figures 4a,b, we show the WAXS data for free-standing films detached from substrates.

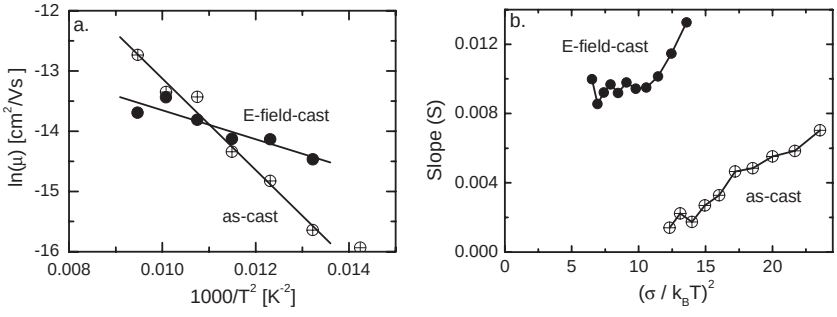

Figure 3. Illustration of the determination of the effective energy (a) and positional disorder (b) parameters from measured TOF data. a) The zero-field mobility is plotted against $1/T^2$ to determine the energy disorder parameter. b) The slope (S in Equation 1) at different temperatures is plotted against normalized energy disorder to determine positional disorder.

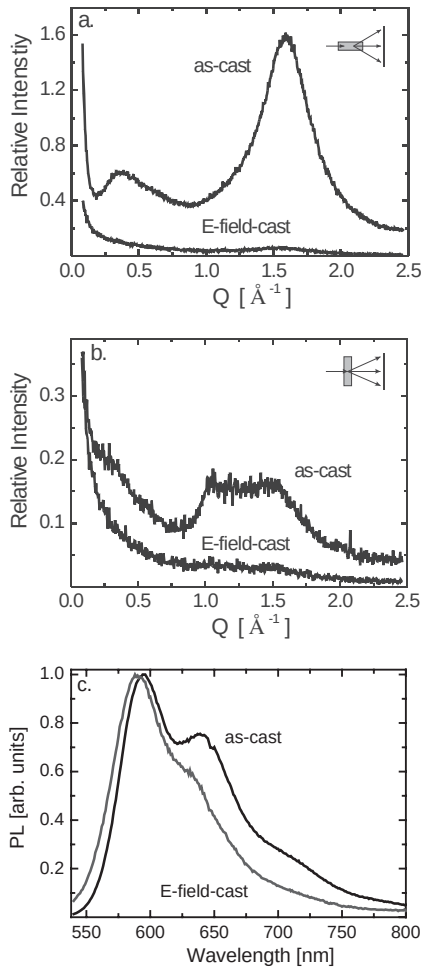

Figure 4. WAXS data for as-cast and E-field-cast films of MEH-PPV as measured in the a) normal-to-plane (perpendicular) direction (charge-carrier-transport direction) and b) in-plane direction. c). Photoluminescence spectra of as-cast and E-field-cast films.

The WAXS data measured both in the in-plane and perpendicular directions of the films exhibit no sharp scattering peaks, indicating a lack of crystalline structure. Nevertheless, the substantial halos observed for the as-cast film in both directions indicate the existence of ordered domains in a largely random polymer network. This ordering gives rise to the local density fluctuations that provide scattering contrast. In the charge-carrier transport direction, the as-cast film shows broadened amorphous halos peaking at $Q = 0.37$ and 1.59 Å^{-1}. The corresponding Bragg-like characteristic *d*-spacings ($d = 2\pi/Q$) obtained from the peak positions are 17.0 Å and 4.1 Å. The domain sizes (D) estimated from the full width at half maximum (ΔQ) of the scattering peaks using $D = 2\pi/\Delta Q$ are ~80 Å and 16 Å, respectively. The characteristic spacing of 4.1 Å corresponds to the benzene-ring packing distance between neighboring polymers, whereas the characteristic spacing of 17 Å corresponds to a possible bilayer structure of MEH-PPV. In the in-plane direction, the WAXS result for the as-cast film shows an additional characteristic length of 6.3 Å at $Q = 1.0$ Å^{-1}. This is assigned to the characteristic length of the monomeric repeat along the backbone of MEH-PPV. From X-ray reflectivity and density measurements, the volume fraction of the ordered domains is estimated as 0.52 ± 0.13; however, a complete analysis of the as-cast film is beyond the scope of this paper and will be published separately. In contrast, the featureless WAXS (Figs. 4a,b) for the E-field-cast film in both in-plane and perpendicular directions imply a completely amorphous structure with no short-range-ordered domains. Clearly, inhomogeneity is reduced by the applied electric field during film formation. It is likely that the interaction between the electric field and polar parts of MEH-PPV prevents any kind of ordered packing during the solvent-drying process. In other words, the interactions between the applied electric field and the polar parts of MEH-PPV are stronger than the van der Waals interactions between individual MEH-PPV polymers that lead to packing.

The photoluminescence (PL) spectrum sheds further light on the nature of the thin films. Figure 4c shows the PL spectra of the E-field-cast and as-cast films. For the PL of as-cast film, the ratio of the relative intensity of the shoulder at 632 nm to the main peak is ~0.77, while that for the E-field-cast film is ~0.6. The lack of a significant shoulder at 632 nm indicates that aggregation has been reduced,[13] and thus is consistent with the WAXS data.

From the TOF and WAXS data, the effect of positional disorder cannot be ignored.[20] Neglecting positional disorder, the greater slope of the room-temperature field-dependent mobility (Fig. 2a) of the E-field-cast relative to the as-cast film would lead one to expect that the E-field-cast film has higher energy disorder. The fact that the E-field-cast film actually has a lower energy disorder indicates the importance of positional disorder in this system. There appear to be two different morphologically based mechanisms responsible for the differences in charge transport between the two types of films. While there are only amorphous-like structures in the E-field-cast films, in the as-cast, partially ordered film, holes are transported through both order-like as well as amorphous-like domains.[16,24,25] These ordered nanometer-sized domains may act as deep traps that are not in good "contact" with the Gaussian density of states of the amorphous regions. In addition, charge mobility may be hindered by the higher fluctuation of site distance and orientation (as shown the difference in positional disorder parameters) in as-cast films relative to the E-field-cast films. Greater spatial homogeneity is thus beneficial to charge transport. Clearly, the present results suggest that the ratio of the two types of regions dominates the overall mobility.

Although the effective energy disorder and positional disorder parameter can be derived from the experimental data within the constructs of the basic GDM, this might not be the best starting point for a complete model of thin films of MEH-PPV. While the homogeneous amorphous structures in the E-field-cast film suggests that Bässler's model should be sufficient in this case, the clear existence of ordered domains as well as the amorphous structures in the as-cast film suggests

ADVANCED MATERIALS

that a model that incorporates spatial inhomogeneity, such as the extension of GDM of Rakhamanova and Conwell[20] or the analytical model of Fishchuk et al.[26] may be a better starting point for a complete understanding of both films.

In conclusion, a hole mobility of $\sim 10^{-5}$ $cm^2 V^{-1}s^{-1}$ with an applied electrical field of 6×10^4 $V cm^{-1}$ has been achieved at room temperature for MEH-PPV. This is one of the highest recorded mobilities for any member of the PPV family. Assuming that evaporation rates can be slowed down, this method may allow the mobility in other polymers with small ordered domains to be increased. It may also be applicable to ink-jet printing. Furthermore, it would be interesting to further investigate the behavior of such films in thin-film transistor geometry.

Experimental

Thin films of ~3.5 μm thickness were prepared via the drop-casting method from 5 $mg mL^{-1}$ of MEH-PPV in CB on pre-cleaned, ITO-coated substrates. The solvent was allowed to vaporize slowly in a solvent-rich atmosphere to get good optical-quality films. During the deposition process, in one group of films, an electric field was applied parallel to the substrate with the ITO being connected to the positive electrode and the negative electrode placed at the other end of the substrate. The schematic diagram is shown in Figure 5. The distance between the negative electrode and the edge of the film was a few millimeters, and the applied voltage could be as high as 5 kV. These

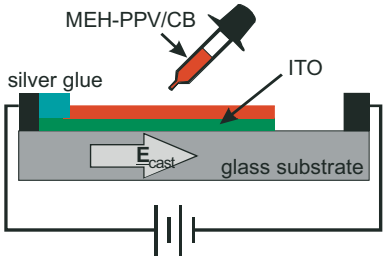

Figure 5. Schematic of the electric-field-processing apparatus.

films are denoted as E-field-cast. In the other group (denoted as as-cast), no electric field was applied. The films were then dried for 24 h at room temperature and the residual solvent was removed by placing the films in a high vacuum chamber. Subsequently, 1000 Å thick aluminum electrodes were thermally evaporated via the shadow-mask procedure to yield the active area of 4 mm^2 for TOF studies. The resulting capacitance of the device was ~30 pF. Using $Q = CV$, a total charge of 1200 pC was estimated at 40 V, where Q is the charge, C is the capacitance, and V is the applied voltage. In order to ensure that the electric field was not perturbed, the injected charge was kept below ~100 pC [14–16].

Temperature-dependent mobility was measured at temperatures ranging from 225 to 325 K. The signal-to-noise ratio and the time resolution of the TOF set-up determined the lowest and highest temperature in this investigation respectively [15]. Both the as-cast and E-field-cast films were prepared from the same solution batch. Experiments were repeated using different polymer batches. In repeated measurements on the same device, no deterioration in mobility of either device was observed over a period of ~2.5 months.

For WAXS measurements, we detached the thin films from the glass substrates. The detached films were then carefully folded into layers of ~120 μm thickness and ~5 mm × 5 mm area. WAXS for the freestanding films were conducted on the diffractometer beamline of BL17A in the National Synchrotron Radiation Research Center (NSRRC), Taiwan. The X-ray beam, monochromated to 1.326 Å, was collimated into a beam size 0.5 mm high and 3 mm wide by two sets of slits separated by 1.1 m. A point detector located 70 cm behind the sample scanned data in a wide Q-range in the polar direction ($Q = 4\pi \sin\theta/\lambda$ where 2θ is the scattering angle and λ the wavelength of the radiation quanta). With sample surfaces perpendicular to the incident beam, we collected in-plane WAXS. With sample surfaces sitting horizontally for a small incidence angle of ~0.3°, we collected WAXS along the perpendicular direction of the films. Owing to the much smaller beam divergence in the vertical relative to the horizontal direction, the WAXS data collected in the Q-regions 0.1–4.5 $Å^{-1}$ in the z-direction were less contaminated by the direct beam profile, compared to the WAXS data collected in the horizontal direction.

Received: February 2, 2005
Final version: April 19, 2005

[1] R. H. Friend, R. W. Gymer, A. B. Holmes, J. H. Burroughes, R. N. Marks, C. Taliani, D. D. C. Bradley, D. A. Dos Santos, J. L. Bredas, M. Logdlund, W. R. Salaneck, *Nature* **1999**, *397*, 121.
[2] C. D. Dimitrakopoulos, P. R. L. Malenfant, *Adv. Mater.* **2002**, *14*, 99.
[3] L. Dai, B. Winkler, L. Dong, L. Tong, A. W. H. Mau, *Adv. Mater.* **2001**, *13*, 915.
[4] H. Sirringhaus, P. J. Brown, R. H. Friend, M. M. Nielsen, K. Bechgaard, B. M. W. Langeveld-Voss, A. J. H. Spiering, R. A. J. Janssen, E. W. Meijer, P. Herwig, D. M. de Leeuw, *Nature* **1999**, *401*, 685.
[5] A. Facchetti, M. H. Yoon, C. L. Stern, H. E. Katz, T. J. Marks, *Angew. Chem. Int. Ed.* **2003**, *42*, 3900.
[6] A. Babel, S. A. Jenekhe, *Adv. Mater.* **2002**, *14*, 371.
[7] A. Babel, S. A. Jenekhe, *J. Am. Chem. Soc.* **2003**, *125*, 13 656.
[8] T. Q. Nguyen, V. Doan, B. J. Schwartz, *J. Chem. Phys.* **1999**, *110*, 4068.
[9] C. H. Tan, A. R. Inigo, W. S. Fann, P. K. Wei, G. Y. Perng, S. A. Chen, *Org. Electron.* **2002**, *3*, 81.
[10] F. Hide, M. A. Diaz-Garcia, B. J. Schwartz, M. R. Anderson, Q. Pei, A. J. Heeger, *Science* **1996**, *273*, 1833.
[11] T. Q. Nguyen, I. B. Martini, J. Liu, B. J. Schwartz, *J. Phys. Chem. B* **2000**, *104*, 237.
[12] C. J. Collision, L. J. Rothberg, V. Treemaneekaran, Y. Li, *Macromolecules* **2001**, *34*, 2346.
[13] R. Jakubiak, C. J. Collison, W. C. Wan, L. J. Rothberg, *J. Phys. Chem. A* **1999**, *103*, 2394.
[14] I. H. Campbell, D. L. Smith, C. J. Neef, J. P. Ferraris, *Appl. Phys. Lett.* **1999**, *74*, 2809.
[15] A. R. Inigo, C. H. Tan, W. S. Fann, Y. S. Huang, G. Y. Perng, A. A. Chen, *Adv. Mater.* **2001**, *13*, 504.
[16] A. R. Inigo, H. C. Chiu, W. S. Fann, Y. S. Huang, U. S. Jeng, T. L. Lin, C. H. Hsu, K. Y. Peng, S. A. Chen, *Phys. Rev. B* **2004**, *69*, 075 201.
[17] H. Bässler, *Phys. Status Solidi B* **1993**, *175*, 15.
[18] B. Hartenstein, H. Bässler, S. Huen, P. Borsenberger, M. V. D. Auweraer, F. C. D. Schryver, *Chem. Phys.* **1995**, *191*, 321.
[19] Y. N. Gartstein, E. M. Conwell, *Chem. Phys. Lett.* **1995**, *245*, 351.
[20] S. V. Rakhmanova, E. M. Conwell, *Appl. Phys. Lett.* **2000**, *76*, 3822.
[21] H. C. F. Martens, P. W. M. Bloom, H. F. M. School, *Phys. Rev. B* **2000**, *61*, 7489.
[22] P. W. M. Blom, M. C. J. M. Vissenberg, *Phys. Rev. Lett.* **1998**, *80*, 3819.
[23] D. Hertel, H. Bässler, U. Scherf, H. H. Horhold, *J. Chem. Phys.* **1999**, *110*, 9214.
[24] C. Y. Yang, F. Hide, M. A. Diaz-Garcia, A. J. Heeger, Y. Cao, *Polymer* **1998**, *39*, 2299.
[25] S. H. Chen, A. C. Su, H. L. Chou, K. Y. Peng, S. A. Chen, *Macromolecules* **2004**, *37*, 167.
[26] I. I. Fishchuk, A. Kadashchuk, H. Bässler, D. S. Weiss, *Phys. Rev. B* **2002**, *66*, 205 208.

